Pd/Ni Synergestic Activity for Hydrogen Oxidation Reaction in Alkaline Conditions

István Bakos[1], András Paszternák[1], David Zitoun[2]

[1]*Institute of Materials and Environmental Chemistry, Research Centre for Natural Sciences, Hungarian Academy of Sciences, 1117 Budapest,*
Magyar tudósok körútja 2., Hungary
[2]*Bar-Ilan University, Department of Chemistry and Bar Ilan Institute of Nanotechnology and Advanced Materials (BINA), Ramat Gan 52900, Israel*

ABSTRACT

The investigation of hydrogen oxidation reaction (HOR) in alkaline conditions has been the subject of a wide interest in the past few years with the rise of alkaline membrane fuel cells (AMFCs). In particular, the quest for the lowest content of platinum group metals (PGMs) in the HOR catalyst is ongoing. In this article, we propose the use of a nanoscale Pd layer partially covering a Ni film to provide the most efficient use of the PGM in the HOR catalyst. The Pd/Ni electrodes were prepared by spontaneous and electrolytic deposition of Pd onto smooth polycrystalline Ni surfaces with different surface compositions. The electrodes were characterized by cyclic voltammetry and atomic force microscopy. Electrocatalytic activity in HOR of the Pd/Ni electrodes was measured in alkaline solution by rotating disc electrode method. In the manuscript, we demonstrate that a Pd coverage as low as 1.5% vs. Ni coverage is sufficient to provide a high current density compared to pure Ni. The current density linearly increases with the Pd coverage up to a Pd coverage of 17%; upon further increase in the Pd coverage, the current density reaches a plateau, i.e. the diffusion limit for the HOR process. The comparison with Pd supported on carbon shows the clear benefit for the bimetallic catalyst.
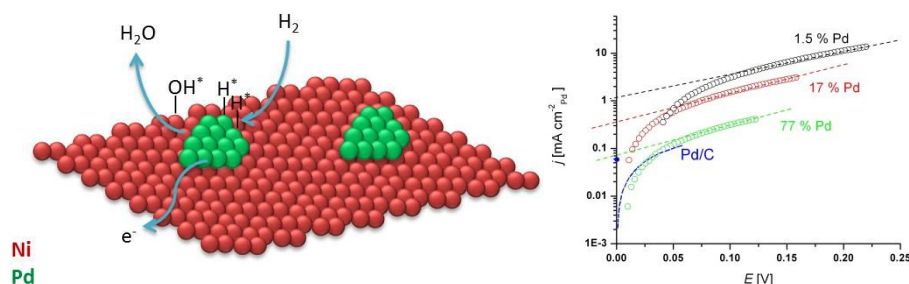
1. Introduction

One of the main drawbacks of the most mature fuel cell technology, the proton exchange membrane fuel cell (PEMFC), is the use of a high Pt content in the membrane electrode assembly (MEA). The cathode electrocatalyst, where the oxygen reduction reaction (ORR) takes place, contains the major ammount of Pt content while the anode electrocatalyst, where the hydrogen oxidation reaction (HOR) occurs, needs a significantly lower ammount of Pt. Indeed, the kinetics of the hydrogen oxidation reaction (HOR) catalysts in acidic conditions for proton exchange membrane fuel cells (PEMFCs) are so fast that the voltage losses at the anode are negligible for platinum group metals (PGMs), focusing most of the research on the ORR.

Alkaline membrane fuel cells (AMFCs) are based on a hydroxide-conducting membrane.[1] After the recent developments in membranes and ORR catalysts,[2] significant barriers remain on the technological roadmap of AMFCs, including development of highly active HOR catalysts with a low content of PGMs.[3] Contrary to PEMFCs, HOR activity in alkaline conditions for alkaline membrane fuel cells (AMFCs) is so poor that it could impede the development of AMFCs, even in the case of Pt. In one of the few studies investigating the HOR activity of platinum in both acidic and alkaline media for several PGMs (Pd, Ir and Pt), the HOR kinetics were found to be at least two orders of magnitude slower in alkaline electrolyte than in acid electrolyte.[4]

On the other hand, AMFCs allow the use of non PGMs catalysts in the less aggressive medium (alkaline, pH = 13) where most of the transition metals form stable solid species.[5] Therefore, the combination of a very low content of active PGM with a low-cost transition metal is very appealing as HOR catalyst in AMFCs. As a typical example, the use of a low amount of Pd, which is a relatively abundant PGM, in combination with abundant transition metals like Ni is very attractive for HOR in alkaline medium.

Palladium, as a pure metal, can be an interesting substitute for Pt anodes in AMFCs. Palladium-based electrocatalysts are intensively investigated as reflected by a recent review.[6] Detailed investigation of HOR activity of polycrystalline palladium in alkaline electrolyte has been published more recently.[7] Synergistic effect of Pd-based alloyed bimetallic catalysts (PdRu, PdIr) or Pd supported tungsten oxide has also been reported for the promotion of HOR activity.[8] Combining palladium with abundant transition metals can be a further step towards higher power and lower cost AMFC anodes.

Nickel is one of the non-noble metals showing attractive performance as electrode material in combination with palladium. PdNi alloys (Pd_3Ni, Pd_3Ni_2) on WC,[9] Pt/Pd, Raney-Ni,[10] were tested in HOR. Various forms of the Pd/Ni bimetallic system were studied as anode for direct ethanol,[11-12] direct methanol,[13] direct glucose fuel cells[14] and in electrooxidation reaction of methanol, ethanol and formic acid.[15-17] Pd/Ni has been investigated as fuel cell cathode for oxygen reduction, as well.[18-19] This large activity on surfaces and dispersed systems of Pd/Ni can be of the utmost interest for the development of HOR electrocatalysts in alkaline medium.

Spontaneous deposition of PGMs on nickel can be carried out via galvanic replacement between Ni and PGMs ions. Other PGMs, like iridium and platinum,[20-21] were deposited by this galvanic replacement reaction (GRR) onto nickel support. GRR offers an extensive control on the surface coverage of the PGM metal on the Ni surface. Such a systematic study has not been carried so far and can provide a clear relationship between the surface coverage and the HOR activity. This type of investigation would then guide the synthesis of high surface area electrocatalysis of the same material, i. e. Pd coated Ni unsupported or carbon supported nanoparticles.

The aim of the present work is to propose a systematic study of the influence of the surface coverage of Pd coated Ni systems, using galvanic displacement as a self limited reaction. In the following, Ni electrodes with a Pd coverage between 1% and 80% have been investigated for their HOR activity.

2. Experimental

Materials: Spectroscopically standardised Ni rod of 5 mm diameter (Johnson Matthey, Specpure) was used for preparing Ni disc electrode. Ni rod was embedded in a PFTE holder, geometric surface area of the electrode (A_g) was 0.2 cm^2. Solutions were prepared from analytical grade chemicals and ultrapure water (Millipore). Sample pretreatment: Ni electrode surface was wet polished with silicon carbide polishing paper (until 4000) and with diamond suspension (6, 3, 1, ¼ μm). After polishing, it was washed with ultrapure water in ultrasound bath and was immediately placed into the electrochemical cell or into the Pd(II) solution.

Pd deposition: 4 x10^{-5} mol dm^{-3} Pd^{2+} (from PdCl$_2$) containing 10^{-3} mol dm^{-3} HCl solution was used for preparation of Pd/Ni electrodes at room temperature (T = 293 K). Three types of Pd deposition were applied:
D1) Spontaneous deposition in open cell without deoxygenation the solution (0.5-40% Pd coverage). Main compartment (round shaped, 45 mm diameter) of the cell was open to the air, without stirring or purging the electrolyte, disc electrode was immersed beneath the solution level by 10 mm.
D2) Spontaneous deposition from deoxygenated solution (0.5-40% Pd coverage). Same procedure as D1 with the difference that the cell was closed and before depositions the electrolyte was deoxygenated with Ar. During the deposition there was no stirring and gas bubbling was stopped.
D3) Electrolytic deposition at controlled potential from deoxygenated solution (>40% Pd coverage). Applied only in combination with D2. After spontaneous deposition for 60 min, potentiostatic deposition was carried our at 90 mV potential. This value was more negative by 10 mV compared to the average of the open circuit potential during the spontaneous deposition in deoxygenated solution. (Open circuit potential was randomly oscillating between 80 and 120 mV during the spontaneous deposition.) There was no stirring during the deposition.
The time of reaction was varied to change the Pd surface coverage on Ni (see table I). After Pd deposition the electrode was rinsed with ultrapure water and surface characterization was carried out.

Morphological characterization: Surface morphology of the sample was studied by atomic force microscopy (Pico, Molecular Imaging, USA). AFM investigations were performed in contact mode in air at room temperature using a commercially available cantilever with a force constant of 0.12 N m^{-1} and Si$_3$N$_4$ tip (Bruker). The roughness profile of the surface was characterized by the area root mean square (RMS), calculated from 6 μm x 6 μm AFM pics with the Gwyddion software.

Electrochemical measurements: Electrochemical measurements were carried out in 0.1 mol dm^{-3} KOH solution, freshly prepared before the experiments. Single-compartment PFTE cell was used in order to avoid the effect of impurities dissolving from glass components. The cell was equipped with two reference electrodes: (i) a Pt/Pt which was used in hydrogen saturated solutions (as hydrogen electrode); (ii) a palladium wire, filled up electrolytically with hydrogen in a separate cell before the experiments. The latter was used as reference in H$_2$-free Ar saturated solutions. All potentials quoted are on RHE-scale. A platinum sheet served as counter electrode. Hydrogen of 99.999 % purity was used in the HOR experiments and 99.9995 % purity argon was used as inert gas.

3. Results and Discussion

3.1 Determination of the electrochemical surface areas

Because of the peculiarities of the two metals, there are no generally accepted, undisputed methods for measuring the real surface area of palladium,[22-23] and nickel electrodes.[24-29] Compared with Pt, Pd exhibits both adsorption and absorption of hydrogen which complicate the calculations of the ECSA from the H-UPD region. CO-stripping is also difficult to apply due to the unknown chemical and crystallographic nature of the surface. Finally, the most accurate but not perfect approximation of the surface area results from the calculations of Ni(III)-Ni(II) and Pd(II)-Pd(0) cathodic peaks. In this work, palladium and nickel surface areas of the Pd/Ni electrodes were calculated from the same voltammograms obtained in 0.1 mol dm^{-3} KOH.

This procedure for the in-situ simultaneous area determination of the two metals can be considered as an estimation. However, since all compared surfaces were the same type having a similar structure and roughness, the relative accuracy of the area calculation is far better and the trends can be described quite well as a result of changing the surface composition. This method has the great advantage that both measurements, surface composition and HOR activity, take place successively in the same cell and same solution, without further experimental manipulation, which could alter the surface.

For the Ni area calculation the Ni(III) - Ni(II) cathodic peak on the same voltammograms was used. Charge corresponding to this peak on the voltammograms with 1500 mV anodic potential limit was calibrated to the Ni/Ni(II) peak at about 300 mV on pure Ni electrode before the measurements of Pd-Ni electrodes. Ni/Ni(II) reaction (Ni $\rightarrow$ α-Ni(OH)$_2$) is reversible when applying +500 mV anodic potential limit on a Ni electrode and frequently used for the surface area measurement of Ni [21-23]. In the presence of Pd this peak overlaps with the oxidation peak of hydrogen sorbed on Pd. Therefore, in

the first step, voltammograms were measured on a freshly polished Ni electrode with -150 and 500 mV potential limits. From the charge corresponding to the reversible oxidation peak (Q^O_{Ni}) the real surface area can be estimated using the usual assumption that charge consumption of this process is 514 $\mu C/cm^2$. According to this calculation roughness factor (R = real surface area/ geometric area) of the polished Ni surface was between 1.9 and 2.1.

In the second step the anodic potential limit of the cyclic polarisation was extended to 1500 mV, into the oxyhydroxide region of Ni, and after stabilization of the shape of the voltammograms (2-3 cycles), the charge corresponding to the NiOOH reduction into β-Ni(OH)$_2$ (cathodic peak at cca 1300 mV) was determined ($Q^R_{Ni(III)}$). The peaks in question are labelled on the voltammograms in Fig 1. Repeating such measurements with Ni electrodes the ratio f = (Q^O_{Ni})/($Q^R_{Ni(III)}$) was 1.4 ±0.06 (averaging from 6 measurements). Thus, applying similar pretreatment (avoiding strong oxidation of the Ni surface before measurement of voltammograms), surface area of Ni (A_{Ni}) can be estimated using $Q^R_{Ni(III)}$ and f:

$$A_{Ni} [cm^2] = f * (Q^R_{Ni(III)}[\mu C]) / 514\ \mu C/cm^2$$

Fig. 2 shows the AFM images of the mechanically polished Ni sample. The morphology of the mechanically polished Ni surface exhibiting relatively large smoothed areas next to some scratches formed during the polishing process.

The composition of a suitable Pd(II) depositing solution was carried out in preliminary experiments. The optimal conditions were achieved through a spontaneous deposition in open cell without deoxigenation the solution. The morphology of the Pd/Ni surface as a function of Pd deposition time has been investigated by AFM. Surface of the Pd coated samples significantly differs from the polished Ni substrate (Fig. 2.). During the spontaneous Pd deposition (performed in open cell) nanosize grains are formed (Fig. 3).

After 30 min deposition (Fig. 3A) grains with a diameter of ~40-50 nm are visible. Although AFM characterization is done separately from the measurements performed in electrochemical cell, 30 min deposition time corresponds to 17% Pd coverage (see Table I.).The grain size distribution is shifted to large size by increasing Pd deposition time. After 60 min (corresponds to 35% Pd coverage) deposition (Fig. 3B), larger grains (diameter: ~120-140 nm) are present next to the smaller grains, observed already after 30 min surface treatment. The formation of the nanosize grains can be attributed to the Pd deposition and Ni dissolution processes taking place simultaneously during the galvanic replacement reaction. The average roughness (RMS) is around 3 nm for the mechanically polished Ni, while its value increases to ~5 nm and ~8 nm after Pd deposition for respectively 30 min and 60 min.

In summary, the average roughness of the electrode did not change significantly during the galvanic replacement. In first approximation, the electrode is consistent with a smooth surface with Pd islands covering a Ni surface.

Pd/Ni electrodes with Pd coverages between about 0.5 % and 40 % could be prepared by spontaneous deposition. Palladium surface area (A_{Pd}) was calculated from the voltammograms assuming that at approximately 1500 mV vs. RHE a complete monolayer oxide is formed and that 424 $\mu C/cm^2$ charge is needed for the reduction of this oxide layer, resulting in an anodic peak at 600 mV vs. RHE.[22-23]

All parameters of the palladization were unchanged except the time of deposition, which was varied between 0.5 min and 120 min. After reaching a certain level of coverage the process of spontaneous deposition slows down. In order to prepare relatively smooth Pd/Ni electrodes with higher palladium coverage other type of Pd depositions were also tested. The same results were obtained when the palladising solution was deoxigenated with Ar before the electroless depositions. In oxygen-free solution, the open circuit potential of the electrode decreased significantly – randomally oscillating between 80 and 120 mV during deposition. Nevertheless, electrodes prepared according to this protocole show the same behaviour as the former set, in oxygen containing solution. Higher Pd coverage could be obtained by a two step procedure. In the first step, electroless spontaneous deposition was achieved as described above and in the second step, potentiostatic deposition was carried out at a potential slightly below the open circuit potential. Electrodes from 40 % up to 80 % Pd coverage could be prepared while their roughness factor remained below 4. (A general roughness factor for Pd/Ni electrodes will be defined in the next paragraph.)

Fig. 4A shows the cyclic voltamogram (CV) in 0.1 mol dm^{-3} KOH of a Ni electrode covered with 8% Pd. The deposition was continued to increase the surface coverage and during this galvanic displacement, the open circuit potential of the electrode varied between 570 mV and 610 mV. Surface area data obtained from the voltammogram are also shown in Fig. 4A. A general roughness factor for the Pd/Ni surfaces was calculated as follows:

$$R= (A_{Pd}+A_{Ni})/A_g$$

where A_g A_{Pd} A_{Ni} are respectively the geometrical, palladium and nickel surface of the electrode.

Fig 4B shows the CV of the same electrode obtained in H_2 saturated KOH and rotating the electrode at 225 rpm. From this curve, the hydrogen oxidation reaction (HOR) started at the low potential value of 50 mV and reached a plateau at around 300 mV. Then, the Pd/Ni activity in the HOR vanished when the Pd was oxidized (above 900 mV) and recovered when PdO was reduced (below 700 mV). The CV shows the anodic polarization (increasing potential) and cathodic polarization (decreasing potential). Except from the HOR activity and the Ni(III)/Ni(II) redox couple, the main feature concerns the irreversible peak at 400 mV in the anodic polarization which can be attributed to the hydrogen oxidation of absorbed hydrogen in the Pd lattice (forming a Pd hydride).

Fig. 5 shows the voltammograms of characteristic Pd/Ni surfaces. There is hardly any observable sign of the palladium in Fig. 5a (0.5 % Pd coverage) and it should be emphasized that in the case of such a low Pd coverage, the estimation of the coverage value is very uncertain. However, it is important to

study this range of composition, as well, because infinitesimal amount of Pd has an exponential effect on the HOR activity.

3.2 Hydrogen oxidation reaction

This non linear enhancement is demonstrated by measuring the HOR activities as a function of Pd coverage, as reported on Fig. 6. All the Pd/Ni rotating disc electrodes were measured in a hydrogen-saturated KOH solution. In Fig. 6, only cathodic polarisation curves were reported to discard the reactivity of absorbed hydrogen and account for the chemisorbed hydrogen only. The coverage values determined previously are annotated on the figure and the polarisation curve of pure Ni RDE is also reported as a comparison (dashed line). Ni RDE does not show any activity in alkaline conditions, which is consistent with a Ni surface covered with oxygen species which inhibits any H adsorption. However, an infinitesimal amount of Pd (0.5 %) coverage immediately activates the Pd/Ni surface. A further increase up to 17% Pd coverage shows two very interesting patterns. The current plateau increases almost linearly from 1.5 % to 17 % Pd coverage while the onset potential non-linearly decreases with increasing Pd coverage. For both trends, a further deposition above 17 % Pd does not improve the values of limiting current and of onset potential. These results clearly demonstrate that the current density values corresponding to the HOR increases steeply with the increasing Pd coverage and reaches maximum at about 17 % coverage. This trend has also been reported on Fig. 6B where the current densities measured at 450 mV in H_2 saturated 0.1 mol dm^{-3} KOH at 1225 rpm are plotted as a function of the Pd coverage for all tested electrodes. Each circle represents Pd coverage surface (more than 20 experiments were carried on). Similar correlation can be observed between the current density and real surface area of the Pd surface (Fig. 6C). The breaking points on the two curves are observed at 17% Pd coverage and 10 mm^2 Pd surface respectively, half of the geometric area of the electrode. At this point, the Pd surface specific current density is near 5 mA cm$^{-2}_{Pd}$.

Figure 7 shows the polarization curves obtained at different rotation speeds on electrodes with a respective Pd coverage of 1.5 % and 17 %. In inset, the current density measured at 450 mV is plotted as a function of the square root of the rotation speed (Levich plot). All samples display a linear Levich plot except for the very low Pd coverage (0.5%) sample. For instance, the 17% Pd coverage displays the typical behavior expected for increasing rotation speeds. More detail features can be observed between 0.1 and 0.2 V which need to be furtherly investigated.

For a more systematic and quantitative evaluation of the electrocatalytic activities of the Pd/Ni electrodes with different surface compositions, the results of the RDE experiments are plotted in a Koutecky-Levich representation in Fig. 8

The linear fit of the Koutecky-Levich plot intercepts the origin in the case of Pd/Ni electrode with 17 % Pd coverage indicating a purely diffusion controlled process. For higher Pd coverage, the same behaviour could be observed for all electrodes and only one further example is shown on Fig. 8 for a better clarity.

Palladium can absorb significant amount of hydrogen. The ratio H/Pd is about 0.6 when the $\alpha \rightarrow \beta$ phase transition is completed and about 0.69 when a palladium electrode is in equilibrium with 1 atm H_2. Oxidation of **ad**sorbed and **ab**sorbed hydrogen takes place in the same potential region; hence, by polarization measurements, the charges associated with the adsorbed (Q^H_{ads}) and absorbed (Q^H_{abs}) hydrogen cannot be distinguished. Only the total charge of sorbed hydrogen ($Q^H_{sorb} = Q^H_{abs} + Q^H_{ads}$) can be measured.

Figure 9 shows the potential sweep measurements of the 17% Pd covered Ni electrode after filling it up with hydrogen. The hydrogen content at the equilibrium could be reached within a short time and there is only a slight difference between the hydrogen oxidation peaks after 20 s and 40 s of hydrogen sorption and the curve after 60 s coincides with the latter.

From the oxidation charge of sorbed hydrogen and reduction charge of surface PdO (Q^O, which was determined from the previous experiment depicted in Fig. 5b) Q^H_{abs} can be calculated (since Q^H_{ads} = $0.5\ Q^O$):

$$Q^H_{abs} = Q^H_{sorb} - 0.5\ Q^O$$

From Q^H_{abs} the amount of deposited Pd can be calculated, since Pd:H atomic ratio is known (0.6). From the number of the bulk Pd atoms and the number of surface Pd atoms we can estimate an average layer thickness which gives the number of atomic layers in the case of uniform distribution. In general, the average number of atomic layers can be given by:

$$N^{Pd}_{av} = \left(\frac{Q^H_{sorb} - 0.5 Q^O}{0.6 * 212} \right) : \left(\frac{Q^O}{424} \right) + 1$$

In this equation instead of number of atoms equivalent Pd surface areas are used:

Q^O (μC) /424 (μC/cm2) is the surface area of Pd (in cm^2).

Q^H_{sorb} - 0.5 Q^O is the charge needed for the oxidation of absorbed hydrogen.

Atomic ratio of Pd_{bulk} : H_{abs} = 1:0.6, hence (Q^H_{sorb} - 0.5 Q^O)/0.6 is the amount of charge if we couple 1 electron to every bulk Pd atoms. Dividing the latter by 212 (μC/cm2) the equivalent surface area can be obtained. (This is the area of equivalent amount of Pd monolayer, when all atoms are on the surface).

According to the results of these calculations for the 17% Pd covered Ni electrode, the Pd loading is around 0.9 μg/cm^2 and the average thickness of the deposit is only 7 atomic layers.

The features of some Pd/Ni electrodes prepared by GRR in an open cell are summarised in Table I. The Pd loading is always found to be very low and corresponds, according to our calculations to several atomic layers thin Pd islands. The thickness of the Pd coating seems to reach a plateau while using GRR as the deposition method, which is consistent with a self-limiting reaction. As pointed above, the HOR activity reaches a maximum for 17% Pd coverage which corresponds to 7 atomic

layers of Pd or a value of around 1.5 nm. The value depends on the growth orientation of the Pd grains and the calculation is based on an arbitrary {111} orientation (d spacing = 0.22 nm). This assumption does not imply that the Pd film displays a single orientation and such a study is not the focus of our investigation.

Indeed, the purpose of this investigation is to understand the limiting factors in the application of Pd/Ni electrocatalysts in HOR oxidation. From the systematic study of 20 samples with different compositions, the threshold for the optimum activity of Pd/Ni is reached for 17% coverage- 1.5 nm thick sample of Pd on Ni. Above these values, no further qualitative or quantitative improvement can be observed in the HOR activity. The loading of Pd reached for this optimized activity is extremely low: 0.9 μg/cm^2 which can be compared with the values obtained on carbon supported Pd catalysts in the same conditions of pH.[30] This publication reports values below 0.1 mA/cm$^2_{Pd}$ at an overvoltage η = 0.05 V for a Pd loading of 5 μg/cm^2. The Pd/Ni with 0.9 μg/cm^2 reported herein reaches 0.30 mA/cm$^2_{disc}$ and 0.57 mA/cm$^2_{Pd}$ at an overvoltage η = 0.05 V (Fig. 10). The Tafel plots show both the Pd/Ni investigated herein and the Pd/C reported in reference.[4] For high Pd coverage on Ni, the exchange current reaches the same value as the Pd/C electrocatalyst. This low values (<0.1 mA/cm$^2_{Pd}$) seem to be typical of pure Pd in alkaline conditions and has been corroborated by the study of Pd covered Au surface.[7] In the case of Pd/Ni, lower Pd coverage allows for much higher values of exchange current, even above 1 mA/cm$^2_{Pd}$ (10 times higher than pure Pd and almost the value of Pt[4]) for a Pd coverage of 1.5% on Ni (Fig. 10).

From the recent literature, the understanding of the reported HOR activity in alkaline environment is still a matter of debate, even for a well-studied system like Pt. Briefly stated, the activity of an HOR electrocatalyst in alkaline medium has been attributed to two main factors: the hydrogen binding energy (HBE) and the oxophilicity of the surface (OH$^-$ binding energy). These statements on single phase catalysts have been argued to be the main factors for the HOR activity and all the litterature agrees on the critical role of the HBE which depends on the electronic structure of the catalyst, and therefore its chemical nature. However, if part of the results tend to corroborate the oxophilic effect in bifunctional bimetallic catalysts,[30-32] some recent results on monometallic oxophilic metals like Ir, show the same trend of HOR decreasing activity from acidic pH to alkaline pH as a non-oxophilic catalyst like Pt.[4] On the other hand, examples have been given for the beneficial effects of surface alloying to HOR rate enhancement in alkaline media, providing both explanations, one based on electronic effects modifying the HBE[33] and the other on added oxophilic function.[32] Such a conclusion may be true for a single metal but the extrapolation to bimetallic surfaces like the Pd/Ni reported in the manuscript may not be accurate. Our results clearly show the benefits of Ni on the HOR rate on Pd. Considering the low temperature synthetic pathway and the scanning probe microscope characterization, the most probable surface composition of the Pd/Ni would be islands of Pd atoms on Ni with limited in-plane and out-of-plane metallic interdiffusion. Therefore, this surface segregation seems much less prone to electronic effects which would be undebatable in the case of alloying and

the role of Ni could be related to its oxophilic character. A better knowledge of the reaction mechanisms still needs to be undergone such as the recent literature on Pt.[34]

4. Conclusions

In this article, a nanoscale Pd layer of around 1.5 nm thickness covering 17% of a Ni film is shown to provide the most efficient use of the platinum group metal in the hydrogen oxidation reaction catalyst. The Pd/Ni electrodes with 20 different Pd coverages were prepared by spontaneous or electrolytic deposition of Pd onto smooth polycrystalline Ni surfaces with different surface compositions. The electrodes were characterized by cyclic voltammetry and atomic force microscopy. Electrocatalytic activity in HOR of the Pd/Ni electrodes was measured in alkaline solution by rotating disc electrode method. A Pd loading as low as 0.9 μg/cm$^2_{disk}$ (17% Pd coverage) is sufficient to reach a diffusion limit for the HOR process. The current density linearly increases with the Pd coverage up to 17%; upon further increase, the current density reaches a plateau, i.e. the diffusion limit for the HOR process. The exchange current reaches values 10 times higher than pure Pd for low Pd coverage on Ni. These results reported can serve as a guideline for the development of an effective Pd supported catalyst by showing the need for a minimal amount of Pd and the optimum for the surface coverage.

References

(1) Lu, S.; Pan, J.; Huang, A.; Zhuang, L.; Lu, J. Alkaline Polymer Electrolyte Fuel Cells Completely Free from Noble Metal Catalysts. *PNAS* **2008**, *105*, 20611–20614

(2) a) Varcoe, J. R.; Atanassov, P.; Dekel, D. R.; Herring, A. M.; Hickner, M. a.; Kohl, P. a.; Kucernak, A. R.; Mustain, W. E.; Nijmeijer, K.; Scott, K.; *et al.* Anion-Exchange Membranes in Electrochemical Energy Systems. *Energy Environ. Sci.* **2014**, *7*, 3135–3191. b) Tang, M. H.; Hahn, C.; Klobuchar, A. J.; Ng, J. W. D.; Wellendorff, J.; Bligaard, T.; Jaramillo, T. F. Nickel-Silver Alloy Electrocatalysts for Hydrogen Evolution and Oxidation in an Alkaline Electrolyte. *Phys. Chem. Chem. Phys.* **2014**, *16*, 19250–19257.

(3) Tang, D.; Pan, J.; Lu, S.; Zhuang, L.; Lu, J. Alkaline Polymer Electrolyte Fuel Cells: Principle, Challenges, and Recent Progress. *Sci. China Chem.* **2010**, *53*, 357–364.

(4) Durst, J.; Siebel, A.; Simon, C.; Hasch, F.; Herranz, J.; Gasteiger, H. A. New Insights into the Electrochemical Hydrogen Oxidation and Evolution Reaction Mechanism. *Energy Environ. Sci.* **2014**, *7*, 2255-2260.

(5) Sheng, W.; Bivens, A. P.; Myint, M.; Zhuang, Z.; Forest, R. V.; Fang, Q.; Chen, J. G.; Yan, Y. Non-Precious Metal Electrocatalysts with High Activity for Hydrogen Oxidation Reaction in Alkaline Electrolytes. *Energy Environ. Sci.* **2014**, *7*, 1719–1724.

(6) Shao, M. Palladium-based Electrocatalysts for Hydrogen Oxidation and Oxygen Reduction Reactions. *J. Power Sources* **2011**, *196*, 2433–2444.

(7) Henning, S.; Herranz, J.; Gasteiger, H. A. Bulk-Palladium and Palladium-on-Gold Electrocatalysts for the Oxidation of Hydrogen in Alkaline Electrolyte. *J. Electrochem. Soc.* **2015**, *162*, F178-F189.

(8) Kwon, K.; Jin, S.; Lee, K. H.; You, D. J.; Pak, C. Performance Enhancement of Pd-based Hydrogen Oxidation Catalysts Using Tungsten Oxide. *Catal. Today* **2014**, *232*, 175–178.

(9) Ham, D.J.; Pak, C.; Hong, G.; Han, S.; Kwon, K.; Jin, S.-A.; Chang, H.; Choic, S. H.; Lee, J. S. Palladium-Nickel Alloys Loaded on Tungsten Carbide as Platinum-free Anode Electrocatalysts for Polymer Electrolyte Membrane Fuel Cells. *Chem. Commun.* **2011**, *47*, 5792–5794.

(10) Kiros, Y.; Schwartz, S. Long-term Hydrogen Oxidation Catalysts in Alkaline Fuel Cells. *J. Power Sources* **2000**, *87*, 101–105.

(11) Miao, F.; Tao, B.; Chu, P. K. Preparation and Electrochemistry of Pd-Ni/Si Nanowire Nanocomposite Catalytic Anode for Direct Ethanol Fuel Cell. *Dalton Trans.* **2012**, *41*, 5055-5059.

(12) Roy, P. S.; Bagchi, J.; Bhattacharya, S. K. The Size-dependent Anode-catalytic Activity of Nickel-Supported Palladium Nanoparticles for Ethanol Alkaline Fuel Cells. *Catal. Sci. Technol.* **2012**, *2*, 2302–2310.

(13) Miao, F.; Tao, B.; Sun, L.; Liu, T.; You, J.; Wang, L.; Chu, P. K. Preparation and Characterization of Novel Nickel–Palladium Electrodes Supported by Silicon Microchannel Plates for Direct Methanol Fuel Cells. *J. Power Sources* **2010**, *195*, 146-150.

(14) Tao, B.; Miao, F.; Chu, P. K. Preparation and Characterization of a Novel Nickel–Palladium Electrode Supported by Silicon Nanowires for Direct Glucose Fuel Cell. *Electrochim. Acta* **2012**, *65*, 149-152.

(15) Miao, F.; Tao B. Methanol and Ethanol Electrooxidation at 3D Ordered Silicon Microchannel Plates Electrode Modified with Nickel–Palladium Nanoparticles in Alkaline. *Electrochim. Acta* **2011**, *56*, 6709– 6714.

(16) Singh, R. N.; Singh, A.; Anindita. Electrocatalytic Activity of Binary and Ternary Composite Films of Pd, MWCNT and Ni, Part II: Methanol Electrooxidation in 1M KOH. Int. *J. Hydrogen Energy* **2009**, *34*, 2052-2057.

(17) Wang, R.; Wang, H.; Feng, H.; Ji, S. Palladium Decorated Nickel Nanoparticles Supported on Carbon for Formic Acid Oxidation. *Int. J. Electrochem. Sci.* **2013**, *8*, 6068 – 6076.

(18) Zhao, J.; Sarkar, A.; Manthiram, A. Synthesis and Characterization of Pd-Ni Nanoalloy Electrocatalysts for Oxygen Reduction Reaction in Fuel Cells. *Electrochim. Acta* **2010**, *55*, 1756-1765.

(19) Li, B.; Prakash, J. Oxygen Reduction Reaction on Carbon Supported Palladium–Nickel Alloys in Alkaline Media. *Electrochem. Commun.* **2009**, *11*, 1162-1165.

(20) Duca, M.; Guerrini, E.; Colombo, A.; Trasatti, S. Activation of Nickel for Hydrogen Evolution by Spontaneous Deposition of Iridium. *Electrocatalysis* **2013**, *4*, 338–345.

(21) Papadimitriou, S.; Armyanov, S.; Valova, E.; Hubin, A.; Steenhaut, O.; Pavlidou, E.; Kokkinidis, G.; Sotiropoulos, S. Methanol Oxidation at Pt - Cu, Pt - Ni, and Pt - Co Electrode Coatings Prepared by a Galvanic Replacement Process. *J. Phys. Chem. C* **2010**, *114*, 5217-5223.

(22) Woods, R. Chemisorption at Electrodes: Hydrogen and Oxygen on Noble Metals and Their Alloys. In *Electroanalytical Chemistry*; Bard, A. J., Ed.; Marcel Dekker: 1976; Volume 9, pp 1.

(23) Grden, M.; Lukaszewski, M.; Jerkiewicz, G.; Czerwinnski, A. Electrochemical Behaviour of Palladium Electrode: Oxidation, Electrodissolution and Ionic Adsorption. *Electrochim. Acta* **2008**, *53*, 7583-7598.

(24) Beden, B.; Floner, D.; Leger, J. M.; Lamy, C. A Voltammetric Study of the Formation on Hydroxides and Oxyhydroxides on Nickel Single Crystal Electrodes in Contact with an Alkaline Solution. *Surf. Sci.* **1985**, *162*, 822-829.

(25) Hahn, F.; Beden, B.; Croissant, M. J.; Lamy, C. In situ UV Visible Reflectance Spectroscopic Investigation of the Nickel Electrode-Alkaline Solution Interface. *Electrochim. Acta* **1986**, *31*, 335–342.

(26) Machado, S. A. S.; Avaca, L. A. The Hydrogen Evolution Reaction on Nickel Surfaces Stabilized by H-Absorption. Electrochim Acta **1994**, *39*, 1385–1391.

(27) Brown, I. J.; Sotiropoulos, S. Electrodeposition of Ni from a High Internal Phase Emulsion (HIPE) Template. *Electrochim. Acta* **2001**, *46*, 2711–2720.

(28) Ganesh, V.; Lakshminarayanan, V. Preparation of High Surface Area Nickel Electrodeposit Using a Liquid Crystal Template Technique. *Electrochim. Acta* **2004**, *49*, 3561–3572.

(29) Hall, D. S.; Bock, C.; MacDougall, B. R. An Oxalate Method for Measuring the Surface Area of Nickel Electrodes. *J. Electrochem. Soc.* **2014**, *161*, H787-H795.

(30) Subbaraman, R.; Danilovic, N.; Lopes, P. P.; Tripkovic, D.; Strmcnik, D.; Stamenkovic, V. R.; Markovic, N. M. Origin of Anomalous Activities for Electrocatalysts in Alkaline Electrolytes. *J. Phys. Chem. C* **2012**, *116*, 22231–22237.

(31) Subbaraman, R.; Tripkovic, D.; Strmcnik, D.; Chang, K.-C.; Uchimura, M.; Paulikas, A. P.; Stamenkovic, V.; Markovic, N. M. Enhancing Hydrogen Evolution Activity in Water Splitting by Tailoring Li$^+$-Ni(OH)$_2$-Pt Interfaces. *Science* **2011**, *334*, 1256–1260.

(32) Strmcnik, D.; Uchimura, M.; Wang, C.; Subbaraman, R.; Danilovic, N.; van der Vliet, D.; Paulikas, A. P.; Stamenkovic, V. R.; Markovic, N. M. Improving the Hydrogen Oxidation Reaction Rate by Promotion of Hydroxyl Adsorption. *Nat. Chem.* **2013**, *5*, 300–306.

(33) Wang, Y.; Wang, G.; Li, G.; Huang, B.; Pan, J.; Liu, Q.; Han, J.; Xiao, L.; Lu, J.; Zhuang, L. Pt–Ru catalyzed hydrogen oxidation in alkaline media: oxophilic effect or electronic effect? *Energy Environ. Sci.* **2015**, *8*, 177-181.

(34) Rheinlander, P.J.; Herranz, J.; Durst, J.; Gasteiger, H.A. Kinetics of the Hydrogen Oxidation/Evolution Reaction on Polycrystalline Platinum in Alkaline Electrolyte Reaction Order with Respect to Hydrogen Pressure *J. Electrochem. Soc.* **2014**, 161, F1448-F1457

Figure captions

Fig. 1. Voltammogams at a sweep rate of 100 mV s^{-1} of the Ni electrode in 0.1 mol dm^{-3} KOH. Potential limits: -150 and 500 mV (insert); -150 mV and 1500 mV; anodic branch of the 1st cycle (dashed red line); stabilized (4th) voltammogram (solid black line). .

Fig. 2: AFM image and cross section profile of Ni polished surface

Fig. 3: AFM images of the Pd/Ni surfaces and size distribution of the grains observed for 17% Pd coverage (A) and 35% Pd coverage (B)

Fig. 4: Stabilized (4th cycle) cyclic voltammogram of a Pd/Ni electrode (8% coverage) in. 0.1 mol dm^{-3} KOH at 100 mV s^{-1} (A) Voltammogram of the same electrode in H_2-saturated 0.1 mol dm^{-3} KOH, rotating the electrode at 225 rpm, sweep rate: 50 mV s^{-1} (B)

Fig. 5. Cyclic voltammogram at sweep rate 100 mV/s for Pd/Ni electrodes with Pd coverage of 0.5 % (A), 17 % (B), 35 % (C), 77 % (D).

Fig. 6. Cathodic polarisation curves of Pd/Ni (solid lines) and Ni (dashed line) RDE in H_2 saturated 0.1 mol dm^{-3} KOH. Rotation rate: 1225 rpm (A); HOR limiting current densities (1225 rpm, 450 mV) vs. Pd coverage (B) and real surface area of Pd (C). Current is normalized to the geometric area of the disc.

Fig. 7: Current density vs. potential curves obtained in H_2-saturated 0.1 mol dm^{-3} KOH at different rotation speeds of a Pd/Ni RDE. Insets: limiting current density vs. $\omega^{1/2}$ plot. Low Pd coverage 1.5 % (A) and optimal Pd coverage: 17 % (B).

Fig. 8: Koutecky-Levich plots of Pd/Ni electrodes derived from RDE measurements at 450 mV in hydrogen saturated 0.1 mol dm^{-3} KOH.

Fig. 9. Potential sweep of the electrode with 17% Pd coverage, obtained in 0.1 mol dm^{-3} KOH (Ar atmosphere) after holding the potential at 30 mV for 20 s (black curve) and for 40 s (red curve). Sweep rate: 50 mV s^{-1}.

Fig. 10: Comparison of the negative going Tafel plot of the HOR kinetic currents normalized to the Pd surface area for three Pd/Ni different coverages with the extrapolated dotted lines and Pd/C from reference [30]

Table I: Characteristics of Pd/Ni electrodes prepared via galvanic replacement by method D1

Figure 1
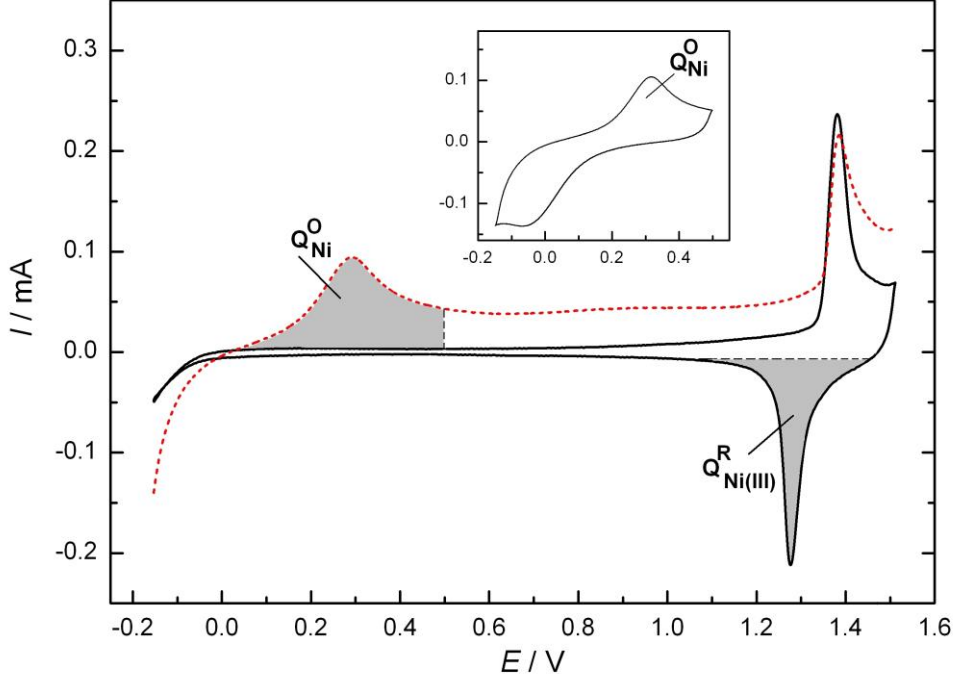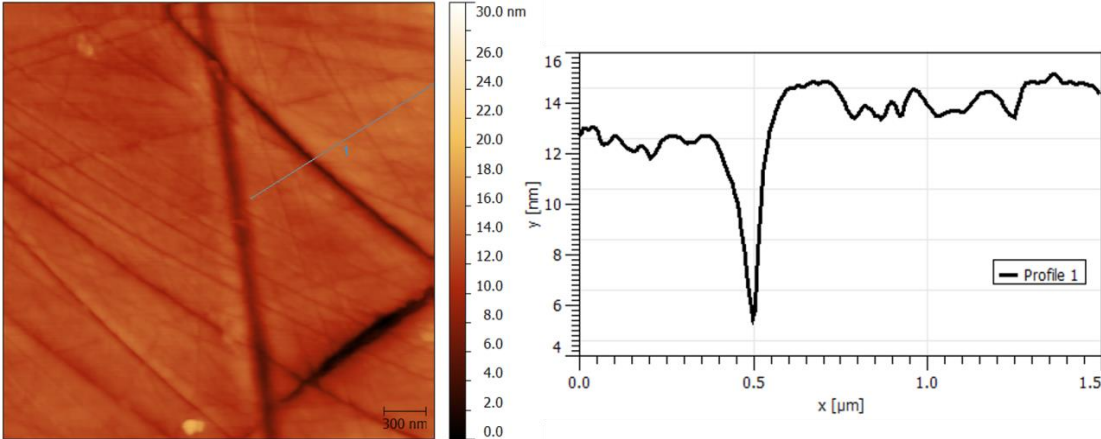

Figure 2

Figure 3
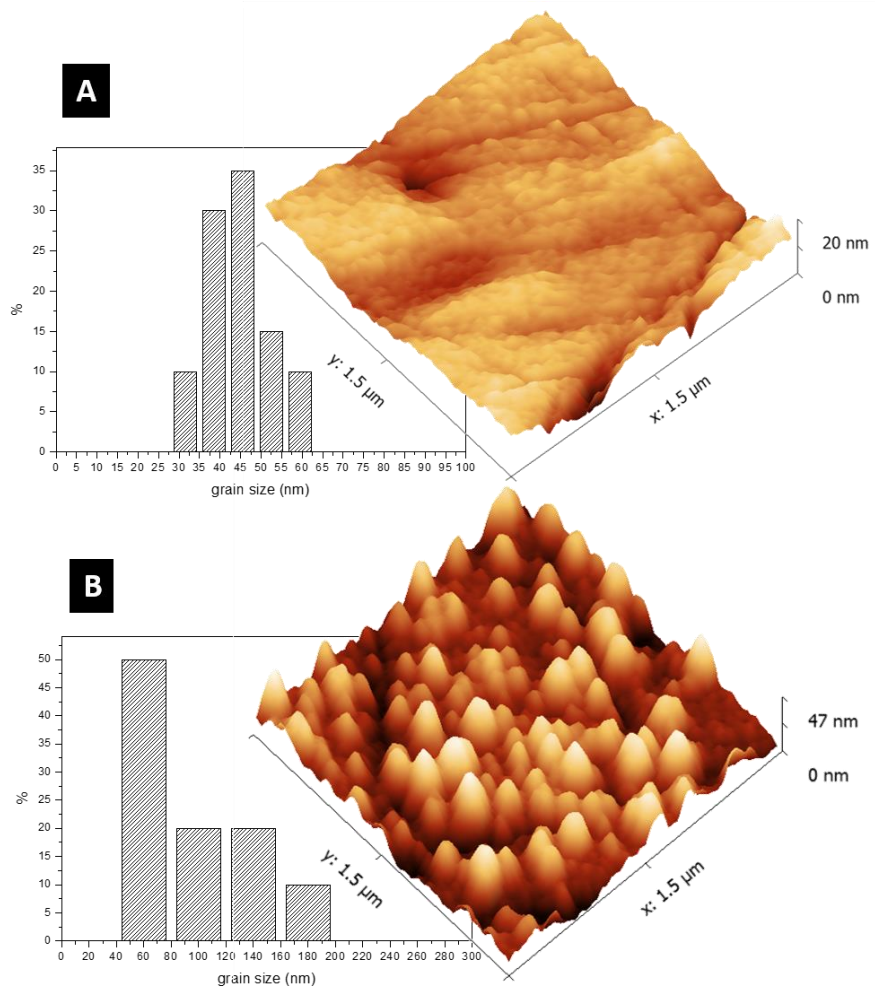
Figure 4
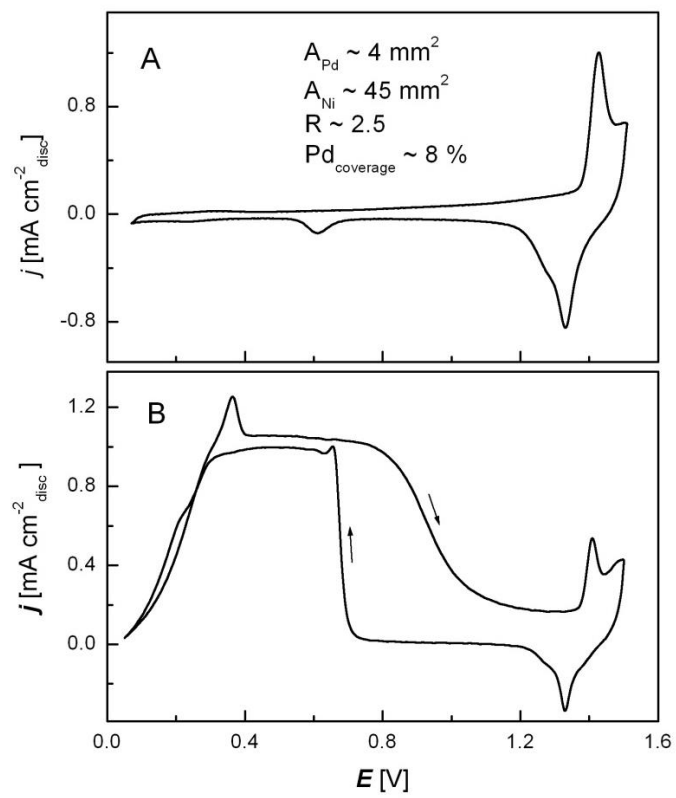
Figure 5
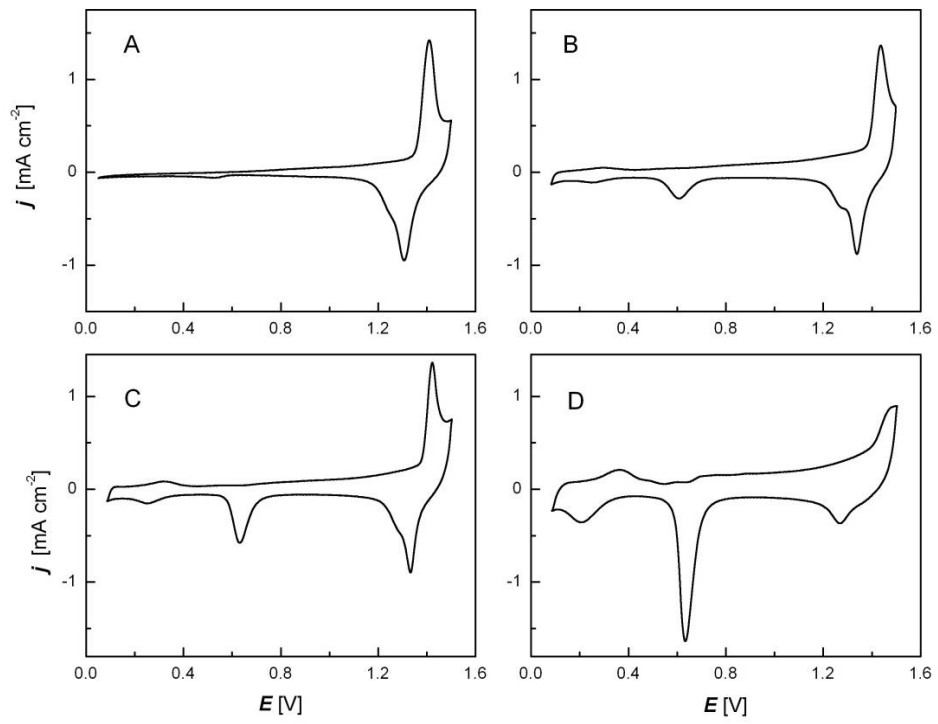
Figure 6
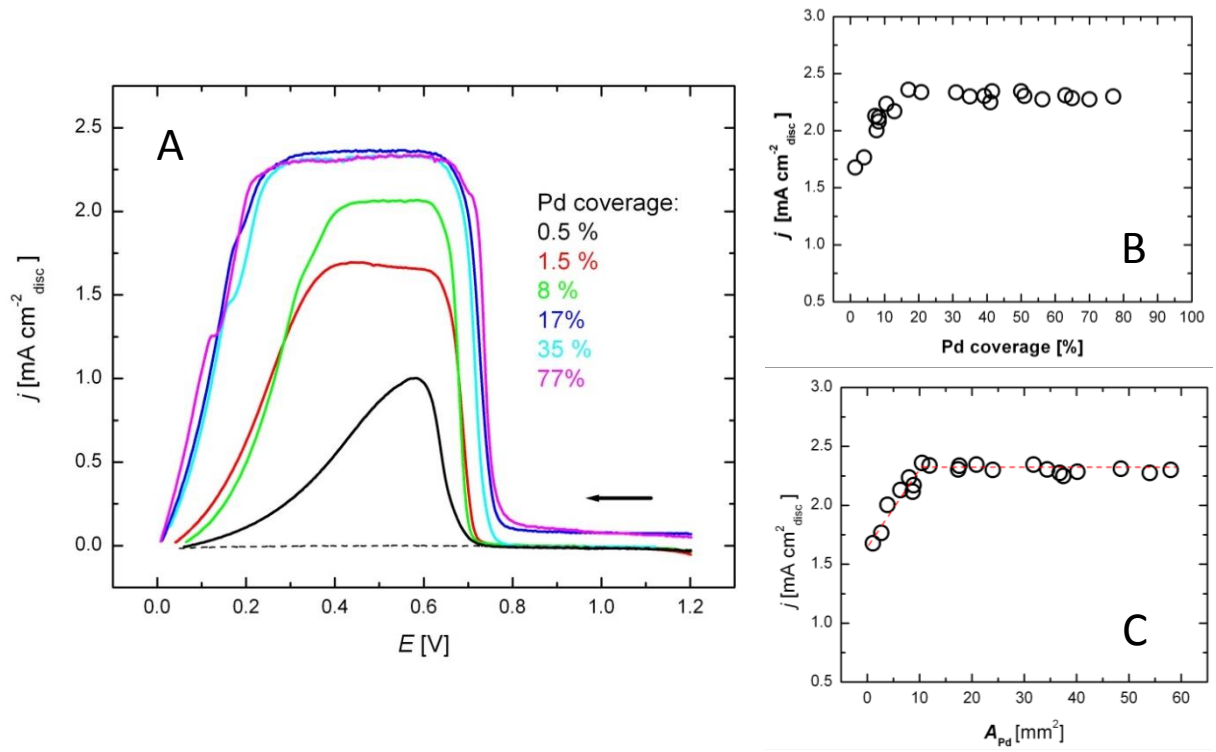
Figure 7
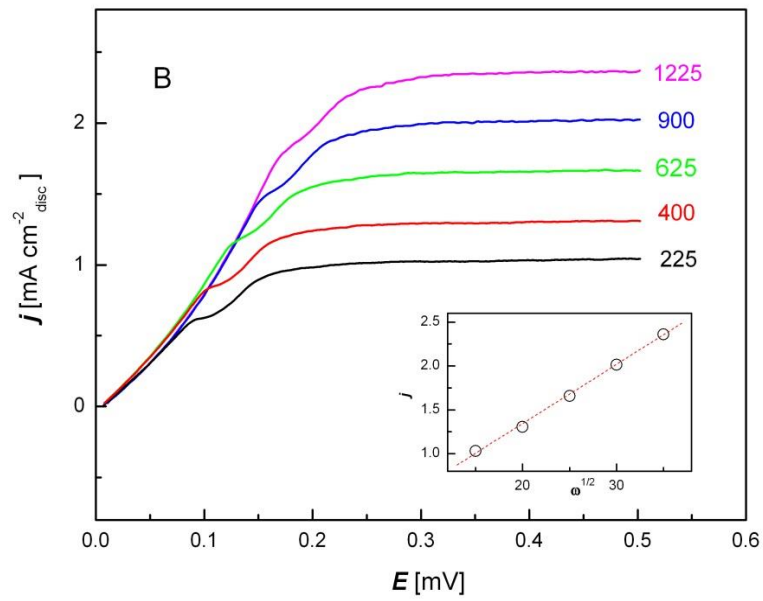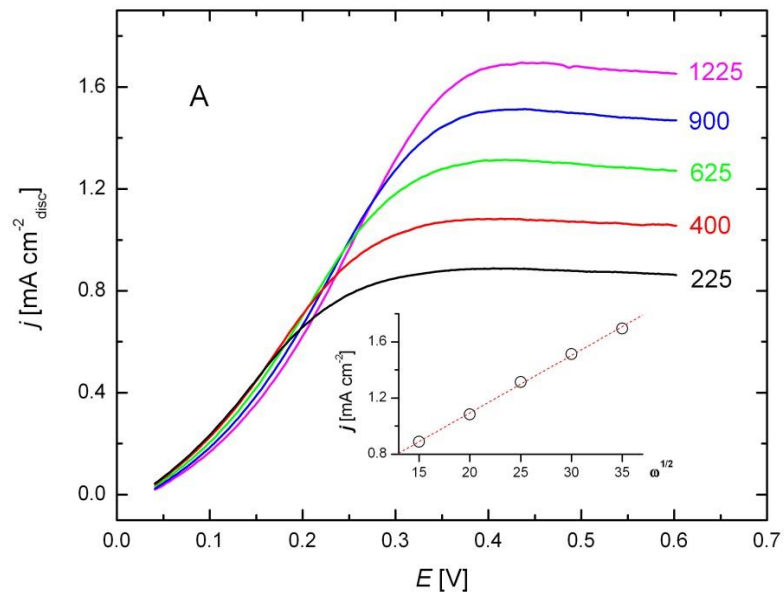
Figure 8
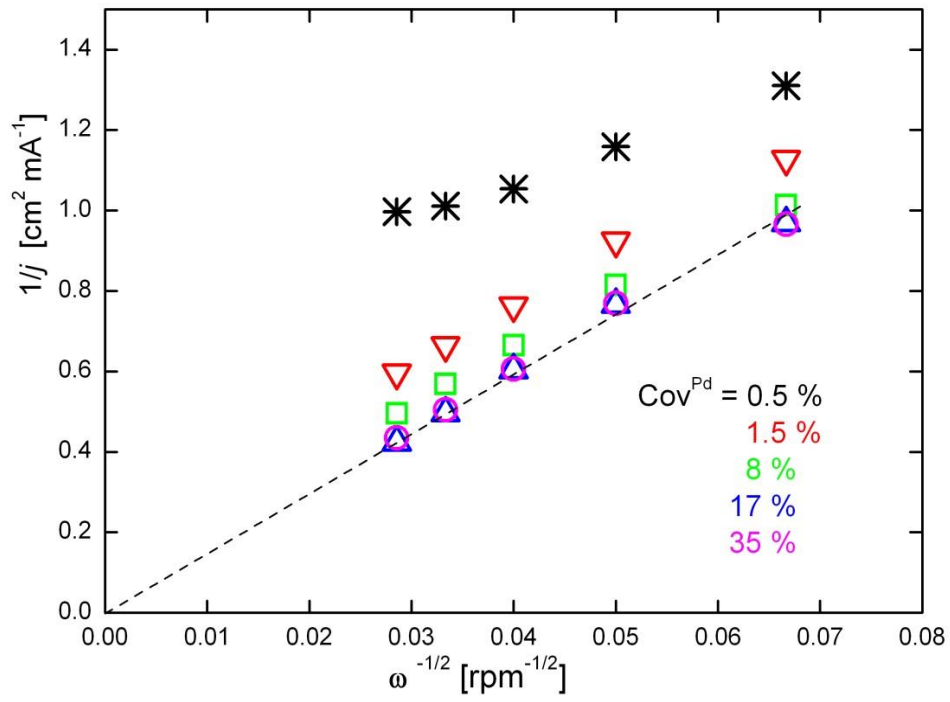
Figure 9
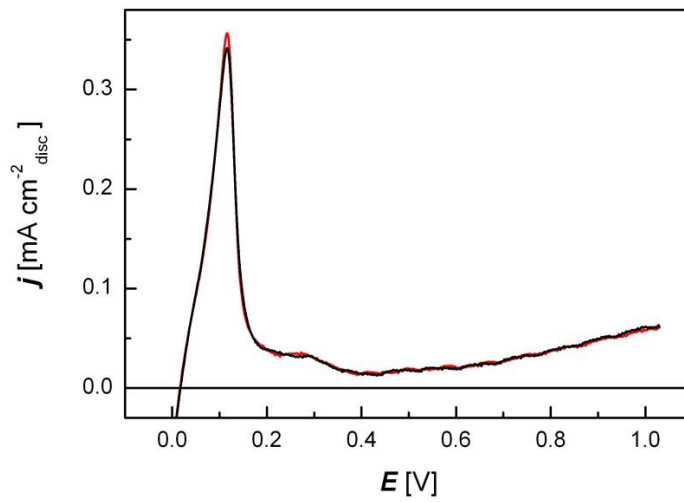
Figure 10
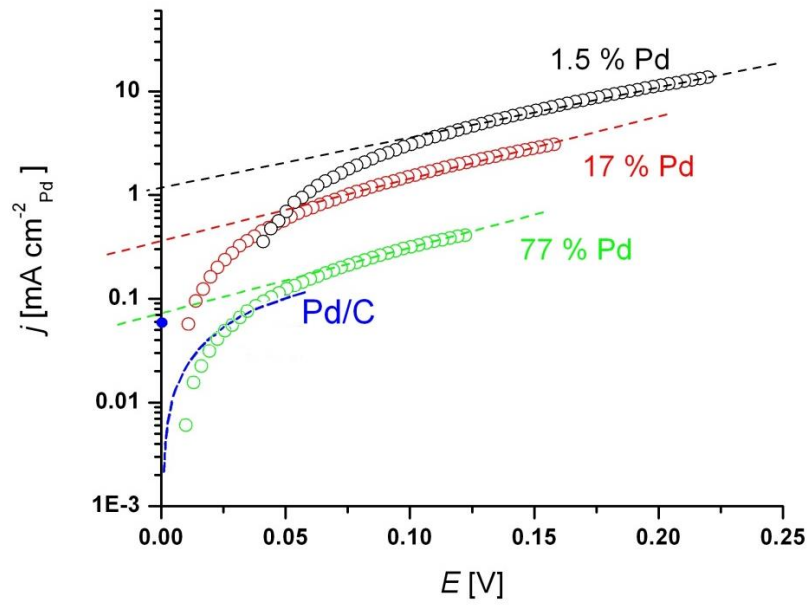
Table 1

Time of deposition [min]	2	10	30	60	120
A_{Pd} [mm^2]	1	4	11	24	38
Coverage = $A_{Pd}/(A_{Ni}+A_{Pd})$ [%]	**1.5**	8	**17**	35	41
Thickness of Pd deposit [atomic layer]	< 2 *	3	7	9	10
Pd loading [$\mu g_{Pd}/cm^2_{disc}$]	< 0.025 *	0.14	0.9	2.5	4.4
HOR current at RDE 1225 rpm, 450 mV, [mA] (I_L)	0.335	0.400	0.472	0.460	0.450
Current density [mA/cm$^2_{disc}$] (I_L / A^g)	1.7	2	2.4	2.3	2.25
Pd surface specific current density [mA/cm$^2_{Pd}$]	30.5	10.3	4.5	1.9	1.2
Pd mass specific current density [mA/μg_{Pd}]	> 68 *	14.3	2.6	0.9	0.5

* not measurable, value of the estimated detection limit is given